Effect of concentration on shear and extensional rheology of guar gum solutions

M.D. Torres[a,b], B. Hallmark[a] and D.I. Wilson[a]

[a]Department of Chemical Engineering and Biotechnology, New Museums Site, University of Cambridge, Pembroke St, Cambridge, CB2 3RA, UK.

[b]Department of Chemical Engineering, University of Santiago de Compostela, Lope Gómez de Marzoa St, Santiago de Compostela, E-15782, Spain.

Submitted to

Food Hydrocolloids

Revised Manuscript

January 2013

Effect of concentration on shear and extensional rheology of guar gum solutions

M.D. Torres · B. Hallmark · D.I. Wilson

Abstract

The steady shear and extensional rheology of aqueous guar gum solutions was studied for concentrations, *C*, ranging from 1 g/L to 20 g/L. Extensional rheometry measurements were made using the Cambridge Trimaster filament-stretching device. The steady shear tests indicated a transition between a semi-dilute regime, below 10 g/L, and an entangled regime at higher concentrations. The solutions were shear-thinning solutions and obeyed the unmodified Cox-Merz rule in the dilute regime, but deviated from Cox-Merz and exhibited strongly viscoelastic behaviour at higher concentrations. The surface tension at higher concentration also deviated from the Szyszkowski model, exhibiting behaviour consistent with entanglement. The filament-thinning data did not fit the model for polymer solution behaviour presented by Entov and Hinch (1997), but gave a good fit to a modified form where time was normalized by the time for filament break-up. This scaling was independent of concentration effects, as reported by Chesterton *et al.* (2011) for cake batters. The modified model parameters approached asymptotic values for entangled solutions. The estimated apparent extensional viscosity exhibited a peak at unit strain followed by a constant value. The former increased as C^n, where $n > 1$, while the latter increased linearly with *C*.

Keywords Elasticity; Extensional; Non-ionic hydrocolloids; Relaxation time; Viscosity

M.D. Torres
Department of Chemical Engineering, University of Santiago de Compostela, Lope Gómez de Marzoa St, Santiago de Compostela, E-15782, Spain.

B. Hallmark (✉)
Department of Chemical Engineering and Biotechnology, New Museums Site, University of Cambridge, Pembroke St, Cambridge, CB2 3RA, UK.
e-mail address: bh206@cam.ac.uk

D.I. Wilson
Department of Chemical Engineering and Biotechnology, New Museums Site, University of Cambridge, Pembroke St, Cambridge, CB2 3RA, UK.

Nomenclature

Roman

a	fitting parameter, Szyszkowski equation, N/m
b	fitting parameter of Szyszkowski equation, g/L
b'	parameter Equation [16], -
Bo	Bond number, -
C	concentration, g/L
c^*	critical concentration, g/L
D_b	diameter at break-up (µm)
D_{mid}	diameter of the filament at midpoint (µm)
D_0	initial sample diameter (µm)
D_1	diameter of the filament when first formed (µm)
F	normal force correction, N
F_{normal}	normal force generated by the flow between plates, N
k	time constant, s^{1-n}
g	gravitational constant, m/s^2
G'	storage modulus, Pa
G''	loss modulus, Pa
L	number of relaxation times, -
M_n	number-average molar mass, g/mol
M_w	weight-average molar mass, g/mol
M_z	higher-average molar mass, g/mol
n	flow index, -
N_1	first normal stress difference, Pa
N_2	second normal stress difference, Pa
N_{Tr}	Trouton number, -
p	probability, -
R_{pp}	radius of parallel-plate geometry, m

R^2	square of the correlation coefficient, -
t	time, s
t_{cap}	capillary time, s
t_{F0}	time to capillary break-up (water), s
t_F	time to capillary break-up, s
T	torque, N m
X	filament shape factor, Equation (5), -

42

Greek

ε	Hencky strain, -
$\dot{\varepsilon}$	Hencky strain rate, s^{-1}
$\dot{\gamma}$	shear rate, s^{-1}
$\dot{\gamma}_R$	shear rate experienced at the rim of the parallel plates, s^{-1}
Γ	surface tension between liquid phase and the air, N/m
Γ_0	surface tension between the solvent and air, N/m
η_{app}	apparent viscosity, Pa s
η_e	estimated apparent extensional viscosity, Pa s
η_0	zero-shear-rate viscosity, Pa s
η_p	polymeric contribution to the viscosity, Pa s
η_s	solvent viscosity, Pa s
$\lvert\eta^*\rvert$	magnitude of the complex viscosity, Pa s
λ	relaxation time, s
ρ	density, kg/m^3
τ	shear stress, Pa
ω	angular frequency, Hz
Ω	angular velocity, rad/s

Introduction

Solutions of water-soluble polysaccharides such as guar gum are widely used as thickeners, stabilisers or gelling agents for food applications as well as in pharmaceutical, biomedical, chemical and cosmetic products (Rosell *et al*., 2007). The molecular interactions between the polymer and water as well as polymer chain length determine the rheology of these solutions; polysaccharide chemical structure and size can, therefore, be exploited to develop new products, control processing quality and optimise the design of process equipment (Durand, 2007).

Guar gum is a galactomannan and one of the most cost effective natural hydrocolloids due to its ready availability and ease of manufacture by extraction from *Cyamopsis tetragonolobus* seeds (Cunha *et al*., 2007). This long-chain polysaccharide biopolymer is highly polydisperse (Sittikijyothin *et al*., 2005), has a semiflexible random coil conformation composed of a linear mannan backbone bearing side chains of a single galactose unit (Imeson, 2010), and contains a mannose to galactose ratio of ~1.6-1.8:1 (Cunha *et al*., 2007). Aqueous guar gum solutions are widely used in food products (*e.g*. Miquelim and Lannes, 2009; Moreira *et al*., 2011) at different concentrations as a thickening and stabilising agent (Duxenneuner *et al*., 2008; Bourbon *et al*., 2010). In contrast to synthetic polymers, guar gum can form highly viscous solutions at low concentrations (< 1%) which are relatively insensitive to pH, addition of electrolytes and heating (Sittikijyothin *et al*., 2005).

As a viscosity modifier, knowledge of the effect of concentration on solution rheology is required for both product and process design (Moreira *et al*., 2011). The shear rheology of aqueous guar gum solutions has been investigated by many researchers who have probed structure-function-property parameters to gain insight into how, for example, molecular structure and solubility affect the resultant solution properties (e.g., Launay *et al*., 1997; Oblonsek *et al*., 2003; Cunha *et al*., 2005; Chenlo *et al*., 2009, 2010). Guar gum solutions usually exhibit non-Newtonian, shear-thinning, behaviour, where the apparent viscosity decreases with increasing shear rate. The apparent viscosity depends mainly on the molar mass while synergistic interactions are determined by the mannose/galactose ratio and the fine structure of the galactomannan chain.

The majority of studies of guar gum rheology have considered shear rheology: relatively few have investigated the extensional rheology of these solutions despite its importance in many food processing operations, consumer perception studies and product quality evaluation (Padmanabhan *et al*., 1995; Bourbon *et al*., 2010). Much of the work on extensional rheology has considered well characterised, model synthetic polymer solutions, and there is little published on the behaviour of systems containing guar gum and its derivatives, besides that by Tatham *et al*. (1995), Duxenneuner *et al*. (2008) and Bourbon *et al*. (2010). Duxenneuner *et al*. (2008) presented a comprehensive study of the shear and extensional rheological properties of hydroxypropyl ether guar gum solutions at concentrations up to 5 g/L. They investigated the effect of concentration on either the characteristic relaxation times or the transient uniaxial apparent extensional viscosities of dilute and semidilute modified guar gum solutions using a capillary breakup extensional rheometer (CaBER) device. Bourbon *et al*. (2010) studied the steady shear and extensional flow of aqueous guar gum solutions with concentrations between 0.39-0.97 g/L. They reported that the break-up time, relaxation time and elastic modulus increased with increasing polymer concentration. These results were confirmed here. The use of these devices to study biopolymers is increasing, including entagled cellulose solutions (Haward *et al.*, 2012) and pitcher plant liquids (Gaume and Forterre, 2007).

This paper presents an investigation of the effects of concentration on the shear and extensional rheology of guar gum solutions, extending previous work undertaken by other researchers by examining a wider range of solution concentrations (1-20 g/L, covering the range from dilute to entangled behaviour), and linking these observations to synthetic polymer solution behaviour. The aim is to improve the understanding of the rheological behaviour of guar gum solutions in extension to allow these materials to be used more efficiently, with reduced development time.

The present work follows on from investigations of bubbly liquids with a non-Newtonian liquid phase (Torres *et al*., 2013) and moderately high bubble volume fractions (25 %), where the presence of a significant number of bubbles gave rise to viscoelastic behaviour that could not be described adequately by the existing literature. Similar findings were reported for cake batters by Meza *et al*.

(2011) and Chesterton *et al*., (2011). The results reported here allow the contribution from the guar gum solutions to the viscoelastic behaviour observed in guar gum-based bubbly liquids to be computed.

Extensional rheology

Measurements of extensional rheology are needed to characterise fluid properties fully (Odell & Carrington, 2006). Experimental investigation of extensional flows is challenging, particularly for viscoelastic materials (Vadillo *et al*., 2012a), partly due to difficulties in creating a purely extensional flow. During a shear deformation, the fluid elements within the material move in the same direction and slide over each other, whereas in extension the fluid elements either move away or towards each other as the material is stretched or compressed, respectively (Entov and Hinch, 1997). Various testing methods are used (Steffe, 1996; Macosko, 1994) and this study employs the filament thinning technique. The relaxation and decay of a necked sample is controlled by a balance between inertial, viscous, elastic, gravitational and capillary forces (Anna and McKinley, 2001).

The extensional viscosity of synthetic polymer solutions is sensitive to molecular weight and extent of long chain branching (Anna and McKinley, 2001). Addition of polymer increases the shear and extensional viscosity of the fluid and promotes viscoelastic behaviour, which can strongly affect filament thinning and break-up mechanisms (McKinley, 2005; Tuladhar and Mackley, 2008; Vadillo *et al*., 2010; Haward *et al*., 2012). There are very relatively few investigations of the effect of concentration on the extensional properties of synthetic polymer solutions. Behaviour analogous to shear rheology is expected, where at higher concentrations the molecules entangle with each other, limiting the length to which the molecule can be extended. Another effect of concentration is the impact of the polymer chain on the flow field itself (Gupta *et al*., 2000). A transition from the dilute to the entangled regime behaviour is therefore expected for guar gum solutions.

Many mathematical approximations for extensional rheology behaviour have been implemented and several closed form constitutive equations exist (Bird *et al*., 1987; Larson, 1988). Most testing has been conducted with shear flows, and the reliability of these equations for strongly extensional

flows, where a substantial degree of stretching is anticipated, is not well understood and the available constitutive equations are not able to predict all the measured transient extensional stresses (Gupta *et al*., 2000).

Materials and Methods

Sample preparation

Commercial guar gum was supplied by Sigma-Aldrich (batch no. 041M0058V, India) with a reported molecular weight of 2.9×10^6 g/mol. The weight-average molar mass (M_w) was determined by gel permeation chromatography (GPC) with a Dawn Heleos-II instrument (Wyatt Technologies) at room temperature, around 21°C, using a PL-aquagel-OH Mixed-H column (7.5 mm × 300 mm, Agilent Technologies), flow rate of 0.5 mL/min, polysaccharide concentration of 0.1% (w/v) with water as the solvent. A differential refractometer was used as the detector. Pullulan samples (Shodex Denko) of M_w 5.9×10^3, 1.18×10^4, 4.73×10^4, 2.12×10^5 and 7.88×10^5 g/mol were used as standards. This yielded a M_w value of 3.0×10^6 g/mol and a small degree of polydispersity, characterised by $M_w/M_n = 1.13$ and $M_z/M_n = 5.15$, where M_n and M_z are the number average molecular weight and higher average molecular weight, respectively.

Aqueous solutions of guar gum at concentrations of 1, 2, 5, 10, 15 and 20 g/L were prepared following the procedure reported by Chenlo *et al*. (2010). The polymer was dispersed in tap water by stirring at 1400 rpm on a magnetic hotplate stirrer (VMS-C4 Advanced, VWR, UK) at room temperature, between 19 °C and 21 °C, overnight to ensure complete hydration of the guar gum. Some air was incorporated into the solution during stirring and deaerated samples of the continuous phase were obtained by centrifugation at 2250 rpm (500 *g*) for 5 min. All samples were, at minimum, duplicated.

Shear rheology

Shear rheological measurements (under steady and oscillatory shear) were performed on a Bohlin CVO120HR controlled-stress rheometer (Malvern Instruments, Malvern, UK) using sand-blasted parallel plates (25 mm diameter and 1 mm gap) to prevent wall slippage. Preliminary tests with

different gap sizes (0.25, 0.5, 0.75 and 1.0 mm) showed good agreement, indicating the absence of significant slip effects. Samples were loaded carefully to ensure minimal structural damage, and held at rest for 5 min before testing to allow stress relaxation and temperature equilibration. A thin film of a Newtonian silicone oil (viscosity 1 Pa s) was applied to the exposed sample edges to prevent evaporation. All measurements were made under isothermal conditions (20 ºC) and, at minimum, duplicated. Error bars corresponding to experiment variation of repeated tests are plotted where the measurement uncertainty was greater than the symbol size.

Steady shear measurements

Viscous behaviour was investigated using steady shear measurements. The apparent viscosity, η_{app}, was determined as function of shear rate, $\dot{\gamma}$, over the range of 0.1 to 1000 s^{-1}. Samples were sheared for 5 s at each shear rate in order to obtain steady-state. Since the shear rate varies with radial position in the parallel plate geometry, the apparent viscosity data were calculated using (Steffe, 1996):

$$\eta_{app}(\dot{\gamma}_R) = \frac{T}{2\pi R_{pp}^3 \dot{\gamma}_R}\left(3 + \frac{d\ln T}{d\ln \dot{\gamma}_R}\right) \quad (1)$$

where $\dot{\gamma}_R$ is the shear rate evaluated at the rim considering angular velocity and geometry, R_{pp} is the radius of the parallel plates and T is the torque. Using linear regression, a relationship between the torque and shear rate data can be obtained in this study, being the slope term defined as $\frac{d\ln T}{d\ln \dot{\gamma}_R}$.

The shear-thinning behaviour of guar gum solutions was fitted to the Cross-Williamson model (Cross, 1965):

$$\frac{\eta_{app}}{\eta_0} = \frac{1}{1 + k\dot{\gamma}^{(1-n)}} \quad (2)$$

where η_0 is the zero-shear rate viscosity, k is the time constant and n is the flow index.

The normal force, F_{normal}, generated by the flow between plates was measured in steady shear tests on the Bohlin rheometer. Measurements of axial thrust were used to estimate the normal stress difference, N_1-N_2 *via* (Steffe, 1996):

$$N_1 - N_2 = \frac{2F_{normal}}{\pi R_{pp}^2}\left(1+\frac{1}{2}\frac{d\ln F_{normal}}{d\ln \dot{\gamma}_R}\right) \quad (3)$$

The normal stress difference data were compared to the computed shear stress and apparent viscosity results to give an indication of when elastic forces became significant. The normal force correction due to inertial effects was estimated using (Kulicke *et al*., 1977):

$$F = -0.075\pi\rho\Omega^2 R_{pp}^4 \quad (4)$$

where Ω is the angular velocity and ρ the liquid density. This force correction was negligible for all tests conducted here.

Oscillatory shear measurements

Viscoelastic behaviour was studied using small amplitude oscillatory shear testing. A strain sweep was performed from 0.01 to 10% at frequencies of 0.01 and 10 Hz prior to each frequency sweep to ensure that tests were performed in the linear viscoelastic (LVE) region for each solution. Frequency sweeps were carried out over the range 0.01 to 10 Hz at a strain amplitude of 1% (well below the LVE limit) and the storage modulus, G', loss modulus, G'', and magnitude of the complex dynamic viscosity, $|\eta^*|$, were determined using the rheometer software.

Extensional rheology

Extensional rheology was investigated using the Cambridge Trimaster, a high-speed filament stretch and break-up device described by Vadillo *et al*. (2010). The apparatus consists of two cylindrical 1.2 mm diameter stainless steel stubs which are moved vertically apart at high speed with high spatial precision. Measurements reported here featured an initial gap spacing of 0.6 mm, final gap spacing of 1.5 mm and piston separation speed of 75 mm s^{-1}. All experiments were performed at least in duplicate in an air-conditioned room at 20 °C.

The filament stretching and thinning profiles were monitored using a high speed camera (Photron Fastcam 1024 PCI) which allows the diameter of the filament midpoint, $D_{mid}(t)$, to be measured to ±0.1 μm at a rate of 6000 frames per second. The device did not feature a force transducer so separating forces were not recorded. Estimates of the apparent extensional viscosity, η_e, can be obtained from the filament regime using (Vadillo *et al*., 2010):

$$\eta_e = (2X - 1)\frac{-\Gamma}{dD_{mid}(t)/dt} \tag{5}$$

where X is a coefficient which accounts for the deviation of the filament shape from a uniform cylinder due to inertia and gravity, Γ is the surface tension between the liquid phase and the air, and t is the elapsed time. Several authors report X values of ~0.7 for polymer solutions at approximately zero Reynolds number (McKinley and Tripathi, 2000; Vadillo *et al*., 2010) whereas X values equalling 0.5912 have been derived by Eggers, 1997 (and further reported by McKinley and Tripathi, 2000) from the universal similarity solution describing the breakup of a Newtonian fluid at non-zero Reynolds numbers. Although the non-zero Reynolds number condition can be shown to be met for the solution containing 1 g/L of guar gum, it introduces an unphysical discontinuity in the trends of extensional viscosity as a function of concentration, presented later, hence X values equalling ~ 0.7 were used in Equation (5).

The equilibrium surface tension between the guar gum solutions and air at 21 °C was determined experimentally using the sessile drop method with a Kruss Drop Shape Analyser 100 device. Values reported are the mean from at least ten measurements.

Filament measurements were obtained using automatic image treatment in the Cambridge Trimaster software. Three characteristic diameters were recorded: D_0, the initial sample diameter, being that of the plates; D_1, the diameter of the filament when first formed, and D_b, the diameter at break-up. The symmetry of the sample during thinning was checked by comparing the filament diameter at positions 100 μm above and below the mid-plane, and asymmetric results discarded. The influence of gravity is characterised by the Bond number:

$$Bo = \frac{\rho g D_0^2}{4\Gamma} \tag{6}$$

where g is the gravitational constant. The sample density was estimated by weighing a 150 mL plastic cup filled with guar gum solution. The surface was levelled off using a spatula, the cup weighed and the density determined as the ratio of the mass of sample to cup volume. The material parameters lie in the range ρ ~ 1086 kg m^{-3}, g = 9.81 m s^{-2}, D_0 = 1.2 mm and Γ ~ 0.067 N m^{-1}, giving Bo values around 0.04. Gravitational effects are therefore expected to be negligible. Transient profiles recorded on the Trimaster for guar gum concentrations of 1 g/L, 10 g/L and 20 g/L can be found in the Supplementary Data.

The Hencky strain, ε, experienced by the sample at the axial midplane at time t is defined using the midfilament diameter:

$$\varepsilon = 2\ln\left(\frac{D_1}{D_{mid}(t)}\right) \tag{7}$$

The apparent extensional viscosity is compared with the apparent viscosity *via* the Trouton number, N_{Tr}. This is the ratio of apparent extensional to shear viscosity at equivalent shear rates, which, for non-Newtonian fluids is given by (Steffe, 1996):

$$N_{Tr} = \frac{\eta_e\left(\dot{\varepsilon}\right)}{\eta_{app}\left(\sqrt{3}\,\dot{\varepsilon}\right)} \tag{8}$$

where $\dot{\varepsilon}$ is the Hencky strain rate. For Newtonian fluids at small strains, N_{Tr} = 3. Departure from this result is due to viscoelastic material behaviour (Steffe, 1996).

Several studies (Bazilevsky *et al.*,1990; Renardy, 1994, 1995; Brenner *et al.*, 1996; Bazilevsky *et al.*, 1997; Entov and Hinch,1997) have presented theoretical treatments predicting the evolution of the midfilament diameter for both Newtonian and viscoelastic fluids. Entov and Hinch modelled the fluid as a FENE material and reported that the midfilament diameter decreased exponentially with time:

$$D_{mid}(t) = \left(\frac{\eta_p D_1^4}{2\lambda\Gamma}\right)^{1/3} \exp\left(\frac{-t}{3\lambda}\right) \quad (9)$$

where $\eta_p = \eta_0 - \eta_s$ is the polymeric contribution to the viscosity (η_s is the solvent viscosity), and λ is the characteristic relaxation time of the polymer.

The analysis above applies to elastic fluids described by a single time constant. However, in reality, polymer solutions can have a spectrum of time constants. Entov and Hinch (1997) showed that for 'intermediate elastic times', *i.e.*, after viscous effects have become negligible relative to elastic effects and before finite extensibility of the dumbbells becomes important, Equation [9] can be generalized to:

$$\frac{D_{mid}(t)}{D_1} = \left(\sum_{i=1}^{L}\left(\frac{\eta_p D_1}{2\lambda_i\Gamma}\right)\exp\left(\frac{-t}{\lambda_i}\right)\right)^{1/3} \quad (10)$$

The second type of characteristic time scale of importance in elasto-capillary thinning studies is the capillary time, t_{cap}, which is the timescale for characterising capillary break-up in viscous Newtonian fluids (Anna and McKinley, 2001). The capillary time quantifies the relative effects of capillary and viscous forces: *viz*.

$$t_{cap} = \frac{\eta_0 D_1}{2\Gamma} \quad (11)$$

where D_1 is used instead of D_0 in this study since the initial filament diameter (D_1) varied widely between notionally identical samples. Similar assumptions were previously made for cake batters with good results (Chesterton *et al*., 2011). Further details of the apparatus and method are given in papers that describe other studies with this instrument (Vadillo *et al*., 2010).

Statistical analysis

Linear and nonlinear regressions were used to extract rheological parameters. The parameters of the models considered were determined from the experimental data with a one-factor analysis of variance (ANOVA) using PASW Statistics (v.18, IBM SPSS Statistics, New York, USA). When the analysis of variance indicated differences among means, a Scheffé test was performed to differentiate means with 95% confidence ($p < 0.05$).

Results and Discussion

Surface tension

The results obtained for aqueous guar gum solutions in Figure 1 shows that the guar gum reduces the surface tension of water, by up to 6 mN m^{-1}. The data exhibit the trend expected for surfactant solutions, albeit with a modest effect. The influence of guar gum concentration was satisfactorily fitted to the Szyszkowski equation (Szyszkowski, 1908):

$$\frac{\Gamma}{\Gamma_0} = 1 - a \ln\left(1 + \frac{C}{b}\right) \tag{12}$$

where Γ_0 is the surface tension of the solvent, C the concentration of the surfactant and a and b are fitting parameters. The data in Figure 1 suggest that the solutions exhibit behaviour associated with the onset of entanglement near 5 g/L, which is in reasonable agreement with the value of 7 g/L reported for other guar gum solutions at 25 ºC by Marangoni and Narine (2002). These surface tension values were consistent with those reported for aqueous guar gum dispersions by Moreira *et al*. (2012).

Steady shear measurements

Flow curves for aqueous guar gum solutions at several concentrations are shown in the form of shear rate sweeps in Figure 2. The apparent viscosity at each shear rate increases noticeably with polymer concentration. In all cases, the solutions exhibit shear-thinning behaviour, where the apparent viscosity decreases with shear rate, and the extent of shear-thinning increases with concentration. Guar gum solutions at concentrations above 5 g/L exhibited strong shear-thinning behaviour, as reported by Chenlo *et al*. (2010); these authors found that the shear rate at which the zero-shear rate viscosity plateau ended depended on polymer concentration, which is also evident in this Figure.

The data gave satisfactory fits (R^2 > 0.996, standard error < 0.032 Pa s) to the Cross-Williamson model, Eqn. [2], and the parameters η_0, k and n obtained are summarised in Table 1. The η_0 and k values increased significantly with increasing polymer concentration, while the variation in n was modest, the values 0.23-0.31 being similar to those reported for synthetic polymer solutions. The

315 increase of η_0 with polymer concentration indicates the establishment of a greater number of links
316 between the biopolymer molecules and depends on the molar mass and on interchain interactions. A
317 higher value of *k* is attributed to an increase in chains entanglement density. Bourbon *et al*. (2010)
318 postulated that the freedom of movement of individual chains is progressively restricted and
319 consequently increases the time needed to form new entanglements to replace those destroyed by the
320 external deformation. Hence, the shear rates values at which the behaviour becomes shear-thinning
321 decrease as the concentration increases, as evident in Figure 2. These results were consistent with
322 those previously found for other guar gum solutions (Chenlo *et al*., 2010; Duxenneuer *et al*., 2008).
323
324 The normal stress difference data, N_1-N_2, presented in Figure 3(a) indicate that aqueous guar gum
325 solutions generate appreciable elastic responses at high shear rates. The normal stress difference, N_1-
326 N_2, for guar gum solutions at 1 g/L was practically negligible, whereas for C = 20 g/L N_1-N_2
327 increased rapidly at shear rates above 1 s^{-1}. This value at which N_1-N_2 increased noticeably was
328 shifted to higher shear rates at lower concentrations. The shear rate at which N_1-N_2 increased
329 corresponds to the onset of noticeable shear-thinning in Figure 2.
330
331 The data in Figure 3(a) are plotted in dimensionless form in Figure 3(b). The normal stress
332 difference is plotted as the approximate Weissenberg number, *Wi* ($Wi = N_1/\tau \approx N_1\text{-}N_2/\tau$) while the
333 shear rate is presented as the dimensionless shear rate suggested by the Cross-Williamson model (the
334 product, $k\dot{\gamma}^n$, which may be interpreted as the rate of link breakage). The data sets follow a
335 common trend, with *Wi* increasing with breakage rate, which merits further investigation. The
336 results confirm that viscoelastic responses can be generated in guar gum solutions under steady
337 shear.
338
339 *Oscillatory shear measurements*
340 Selected mechanical spectra (*G'* and *G"* vs. angular frequency) of aqueous guar gum solutions
341 prepared at several concentrations are presented in Figure 4. The elastic modulus, *G'*, related to the
342 elastic response of the system, and the viscous modulus, *G"*, related to the viscous response of the
343 system, increased at low frequency by roughly five orders of magnitude with increasing polymer

concentration. The mechanical behaviour of the guar gum solutions was dependent on frequency and followed the shape reported elsewhere for similar guar gum solutions (Steffe, 1996; Chenlo *et al.* 2010). In all cases, both moduli increased with frequency by roughly three orders of magnitude between 0.01 and 10 Hz. For low polymer concentrations below 5 g/L, *G"*>*G'* over the entire frequency range investigated, indicating predominantly viscous behaviour (Figure 4a), whereas there is a crossover in the moduli at higher concentration (above 10 g/L) and the elastic response prevails at higher frequencies (Figure 4b). These results are similar to those reported for random coil polymers. The crossover frequency (where *G*'~ *G"*) decreased from 4 Hz to 1 Hz as the concentration increased from 10 g/L to 20 g/L, as a consequence of longer relaxation times. Bourbon *et al*. (2010) reported similar behaviour for several other random-coil polysaccharide solutions in this concentration range. The viscoelastic behaviour of the guar gums solutions was predominantly viscous over the range of angular frequencies for other concentrations, indicating that the entangled regime is encountered between 5 and 10 g/L.

Complex viscosity

Figure 5 shows that the solutions obeyed the Cox–Merz rule, $\left|\eta^*(\omega)\right| \approx \eta(\dot{\gamma})$ where $\omega = \dot{\gamma}$, (Cox and Merz, 1958), relating the apparent viscosity (steady shear flow) and the magnitude of the complex viscosity (oscillatory shear flow) at a given frequency and shear rate at concentrations below 10 g/L. There is a divergence in behaviour at high rates for the more concentrated solutions, which are thought to lie in the entangled regime. The deviation is related to the elastic gel-like structure, which is not affected during oscillatory measurements, but is broken during steady shear tests such that the measured magnitude of the complex viscosity is larger than the apparent viscosity (Steffe, 1996). Similar behaviour has been reported for synthetic polymers such as polyisobutylene by Liang and Mackey (1994), who also found that the largest deviations occurred at higher angular frequencies and shear rates.

Extensional measurements

Figure 6 shows the evolution of mid-filament diameter, D_{mid}, for different concentrations. The diameter is determined by the balance of surface tension and viscous/elastic forces: viscous forces

tend to stabilize the filament, while surface tension acts to destabilize it, causing the increasingly rapid decrease in the diameter until the filament breaks apart. The decrease in D_{mid} with time is not linear: there is a sharp step followed by an exponential decay, after which the rate of decay increases towards break-up at time t_F. Similar trends were reported for other aqueous guar gum systems at different concentrations (Duxenneuner *et al*., 2008; Bourbon *et al*., 2010), and confirm non-Newtonian behaviour.

The time to break-up, t_F, increased with polymer concentration and Figure 7 shows that an asymptote is reached around 10 g/L. The effect of concentration, C, on t_F fitted the empirical expression:

$$t_F - t_{F0} = 1 - \exp\left(\frac{C}{20}\right) \tag{13}$$

where t_{F0} is the break-up time observed with water. The square of the correlation coefficient, R^2, was 0.995. This behaviour is consistent with the results obtained for the shear rheology, suggesting that above 10 g/L guar gum solutions lie in the entangled region. The t_F values also increased with D_1 (see the inset on Figure 7), following an exponential dependency given by:

$$t_F = 15.2\exp\left(0.0042D_1\right) \tag{14}$$

with the square of the correlation coefficient, R^2, being 0.998. A similar dependency between t_F and D_1 was reported for cake batters by Chesterton *et al*. (2011).

The individual data sets in Figure 6 collapsed to a common form when the capillary diameter, normalised against D_1, as in Equation (16), was plotted against the timescale was normalised against t_F (see Figure 8):

$$\frac{D_{mid}(t)}{D_1} \propto exp\left(\frac{-t}{t_F}\right) \tag{15}$$

The data sets were also analysed in the form employed by Anna and McKinley (2001) to present data obtained for Boger fluids, namely plots of $[D_{mid}(t)/D_1]$ *vs*. $[t/t_{cap}]$. These plots showed an initially linear region, characteristic of viscoelastic behaviour, followed by a sharp descent towards

filament break-up at t_F (data not presented). The time scaling showed that the decay timescale and the approach to break-up are not determined by the characteristic capillary time. Deviations from the simple form expected for a dilute polymer solution as discussed by Anna and McKinley (2001), were reported for another complex entangled biopolymeric system, cellulose in ionic liquid solutions, using a CaBER device by *Haward et al.* (2012). These authors showed very similar trends for the shear viscosity, linear viscoelastic and extensional data as the present work.

Anna and McKinley (2001) successfully fitted their data for synthetic polymer solutions to Equation (9), relating the observed behaviour to polymer relaxation times and the finite extensibility of polymer molecules. In the current study, however, poor agreement was obtained when experimental data were fitted to Equation (9), with one relaxation time, or to Equation (10) using up to eight relaxation times, as illustrated by the example in Figure 9. An alternative physical mechanism is operating, which is consistent with those observations made by Tembely et al. (2012) and Vadillo et al. (2012), where computational fluid dynamic simulations for predicting the fast filament stretching, relaxation and break up of low viscosity weakly elastic fluids were presented. The authors of this work have also tried mono and multi mode approach to fit the filament thinning of such fluids, rather unsuccessfully, using Oldroyd-B and FENE-CR constitutive equations.

Equation (9) was modified by the addition of an empirical constant, *b*', which yielded a significantly better fit to the experimental data (see Figure 9):

$$\frac{D_{mid}(t)}{D_1} = \left(\left(\frac{\eta_p D_1}{2\lambda_1 \Gamma} \right) \exp\left(\frac{-t}{\lambda_1} \right) \right)^{1/3} - b' \qquad (16)$$

Chesterton *et al*. (2011) reported that their cake batter data fitted this empirical relationship for several different flours.

All the data sets fitted the expression shown in Equation (16) satisfactorily (R^2 > 0.990). The empirical model proposed in Equation (16) exhibits the form expected for a Giesekus fluid (as reported by Yesilata *et al.*, 2006); further exploration of this relationship is currently ongoing. The

relaxation times and *b*' values obtained are presented in Figure 10. The relaxation times increase with increasing polymer concentration, approaching an asymptotic value of 17 ms around 10 g/L, whereas the *b*' values decrease with concentration, approaching an asymptotic value of unity at 10 g/L. Bourbon *et al*. (2010) reported the existence of two relaxation times for aqueous guar gum solutions with values ranging from $\lambda_1 \sim 15$ ms and $\lambda_2 \sim 1$ ms for 1.9 g/L, to $\lambda_1 \sim 58$ ms and $\lambda_2 \sim 4200$ ms for 9.7 g/L. These data can be contrasted against those from this study where the relaxation time, λ_1, ranges between $\lambda_1 \sim 8$ ms for 2.0 g/L and $\lambda_1 \sim 17$ ms for 10 g/L. Bourbon *et al*. (2010) proposed that the two relaxation times arise from the structure of the studied polysaccharides, one related to the expansion of the polymeric chains, the other relating to interactions between the chains delaying the relaxation phase.

Duxenneuner *et al*. (2008) studied modified guar gum solutions and reported that the relaxation time followed a power-law scaling dependency in the semi-dilute concentration regime, from $3c^*$ up to $9c^*$. These authors defined c^* as the critical micelle concentration, which can be identified as the concentration where the surface tension data as a function of concentration deviate from the Szyszkowski equation (Szyszkowski, 1908) that was given in Equation (12); they found that $c^* \sim 0.58$ g/L. These authors stated that this behaviour was a manifestation of increasing interactions between hydroxypropyl ether guar gum molecules in solution with increasing concentration. The relative weak dependency suggests that the interactions between chains were overall quite weak and may be purely hydrodynamic in nature. We note that Haward *et al*. (2012) recently reported a strong dependency of relaxation times with concentration of cellulose in an ionic liquid. They found that the relaxation times obtained from CABER measurements initially increase slowly with concentration and then climb more rapidly in the semi-dilute and entangled regimes.

Figure 11 shows that t_F exhibits a linear dependency on the relaxation time parameter, λ. No further explanation is offered at this time as the physical basis of Equation (16) is not established.

The apparent extensional viscosity was estimated using Equation (5) and the results are presented in Figure 12. This analysis assumes that the equilibrium surface tension values in Figure 1 can be used

457 to estimate the forces involved in extension; direct measurement of the force in the filament is
458 required to confirm these values. Figure 12(a) plots the apparent extensional viscosity as a function
459 of the Hencky strain. Since the apparent extensional viscosity profiles are a function of the
460 midfilament diameter, D_{mid}, which itself changes as a function of time, the values are governed by
461 the self-thinning of the filament, and are not a response to an imposed shear rate as in shear
462 rheometry. The apparent extensional viscosities increase sharply at low Hencky strains, exhibiting a
463 peak (at $\varepsilon \sim 1.2$) for concentrations above 10 g/L, where entanglement is believed to be important.
464 At higher strains, η_e approaches an asymptote, the value of which increases with concentration.
465
466 The effect of concentration on the peak and plateau values of the apparent extensional viscosity is
467 presented in Figure 12(b). Both parameters increase with concentration, with the plateau value
468 following a linear dependency but the peak value exhibiting an exponential dependency.
469 Duxenneuner *et al*. (2010) reported two steady-state extensional trends for hydroxypropyl ether guar
470 gum solutions: a linear dependence of the plateau values up to ~3 times the critical polymer
471 concentration (c^* ~ 0.58 g/L), followed by a power-law dependence up to their highest-studied
472 concentration (around 1 g/L) of ~9 times the critical polymer concentration.
473
474 The apparent extensional viscosities are now compared with the apparent viscosities via the Trouton
475 number (*i.e.*, η_e/η_{app}) evaluated at $0.1 s^{-1}$. Figure 13(a) shows the Trouton number values calculated
476 for aqueous guar gum solutions against the Hencky strain. An exponential increase in the Trouton
477 number with Hencky strain was observed in all cases. Moreover, the Trouton number decreased
478 noticeably with an increase of polymer concentration (Figure 13(b)). This trend is consistent with
479 those reported for derived guar gum solutions by Duxenneuner *et al*. (2010), who found that the
480 Trouton number values started as high as 440 for 0.1 g/L and decreased to 16 for 5 g/L over a shear
481 rate range between 0.1 s^{-1} and 1000 s^{-1}. They stated that the high values of Trouton number recorded
482 at the lowest polymer concentration indicate that most of the extensional response is due to the
483 alignment and extension of individual chains, with increasing effects of chain-chain interactions at
484 higher polymer contents.
485

Conclusions

The shear and extensional rheology of aqueous solutions of guar gum with concentrations has been studied over the range 1 g/L to 20 g/L. The molecular weight of the guar gum was 3.0×10^6 g/mol, with a polydispersity (M_w/M_n) of 1.13. The behaviour of the guar gum solutions was predominantly viscoelastic, with the extent of the viscoelasticity being determined by polymer concentration. At concentrations below 10 g/L, the rheological behaviour was consistent with the polymer being in a non-entangled state, but at concentrations above 10 g/L the data suggested the presence of entanglement and the formation of an elastic, gel-like, structure. The measured surface tension values also exhibited behaviour reminiscent of micelle formation at concentrations in the entangled regime.

The steady shear data fitted the Cross-Williamson model well and suggests that shear thinning arises from breakdown of interactions between polymer strands. The viscoelastic response accompanying breakdown, quantified by the first normal stress difference, coincided with the onset of noticeable shear-thinning. Plots of the estimated Weissenberg number against the normalised shear rate calculated from the Cross-Williamson model showed a common trend which merits further investigation.

The filament stretching data did not fit the model presented by Entov and Hinch (1997) which has been successfully used by several workers to describe the extensional behaviour of synthetic polymer solutions, even when eight relaxation times were used. An empirical modification of the Entov and Hinch model, adding a time-independant constant, however, gave good fits with only one relaxation time. This empirical modification exhibits the form expected for a Giesekus fluid, as reported by Yesilata *et al.*, 2006; further exploration of this relationship is ongoing. Plots of the normalised filament diameter against normalised time showed a consistent trend which was largely independent of polymer concentration. This allows a coarse prediction of expected behaviour, and was also reported by Chesterton *et al*. (2011) for cake batters. The apparent extensional viscosity of the guar gum solutions was estimated by monitoring the evolution of solution filament diameter as a function of time using the method reported by Vadillo *et al*., 2010. For dilute solutions, below 10

g/L, the apparent extensional viscosity increases monotonically as a function of Hencky strain, reaching a steady asymptotic value. The apparent extensional viscosity of the entangled solutions also reaches a steady asymptote at high Hencky strain, but passes through a maximum value prior to the asymptote. The asymptotic value of the apparent extensional viscosity is linearly proportional to polymer concentration for both dilute and entangled regimes, with a squared correlation coefficient of 0.995. The peak apparent extensional viscosity, however, increases exponentially across the two regimes as a function of polymer concentration with a squared correlation coefficient of 0.990.

Acknowledgements

The authors acknowledge the financial support (POS-A/2012/116) from Xunta de Galicia's Consellería de Cultura, Educación e Ordenación Universitaria of Spain and European Union's European Social Fund. We also wish to thank Dr Oren Scherman and Louisa Jane Quegan for polymer chain length measurements, Tao Wang for his assistance with the surface tension measurements, Dr Simon Butler for his help with the rheology experiments and Prof. Francis Gadala-Maria for useful discussions.

References

Anna, S. L., & McKinley, G. H. (2001). Elasto-capillary thinning and breakup of model elastic liquids. *Journal of Rheology*, *45*, 115-138.

Bazilevsky, A. V., Entov, V. M., & Rozhkov, A. N. (1990). Liquid filament microrheometer and some of its applications. In D.R. Oliver (Eds.), *Third European Rheology Conference* (pp. 41-43). New York: Elsevier.

Bazilevsky, A. V., Entov, V. M., Lerner, M. M., & Rozhkov, A. N. (1997). Failure of polymer solution filaments. *Polymer Science*, *Series A, 39*, 316-324.

Bird, R. P., Curtiss, C. F., Armstrong, R. C., & Hassager, O. (1987). *Dynamics of Polymeric Liquids*. (2nd ed.). New York: Wiley-Interscience, (Volumen 2: Kinetic Theory)

Bourbon, A. I., Pinheiro, A. C., Ribeiro, C., Miranda, C., Maia, J. M., Teixeira, J. A., & Vicente, A. A. (2010). Characterization of galactomannans extracted from seeds of *Gleditsia triacanthos* and *Sophora japonica* through shear and extensional rheology: Comparison with guar gum and locust bean gum. *Food Hydrocolloids*, *24*, 184-192.

Brenner, M. P., Lister, J. R., & Stone, H. A. (1996). Pinching threads, singularities and the number 0.0304. *Physics Fluids*, *8*, 2827-2836.

Chenlo, F., Moreira, R., Pereira, G., & Silva, C. (2009). Rheological modelling of binary and ternary systems of tragacanth, guar gum and methylcellulose in dilute range of concentration at different temperatures. *LWT - Food Science and Technology*, *42*, 519-524.

Chenlo, F., Moreira, R., & Silva, C. (2010). Rheological properties of aqueous dispersions of tragacanth and guar gums at different concentrations. *Journal of Texture Studies*, *41*, 396-415.

Chesterton, A. K. S., Meza, B. E., Moggridge, G. D., Sadd, P. A., & Wilson, D. I. (2011). Rheological characterisation of cake batters generated by planetary mixing: elastic versus viscous effects. *Journal of Food Engineering*, *105*, 332-342.

Cox, W. P., & Merz, E. H. (1958). Correlation of dynamic and steady flow viscosities. *Journal of Polymer Science*, *28*, 619-622.

Cross, M. M. (1965). Rheology of non-Newtonian fluids: a new flow equation for pseudoplastic systems. *Journal of Colloid Science*, *20*, 417-437.

Cunha, P. L. R., Castro, R., Rocha, F., Paula, R. C. M., & Feitosa, J. (2005). Low viscosity hydrogel of guar gum: preparation and physicochemical characterization. *International Journal of Biological Macromolecules*, *37*, 99–104.

Cunha, P. L. R., de Paula, R. C. M., & Feitosa, J. P. A. (2007). Purification of guar gum for biological applications. *International Journal of Biological Macromolecules*, *41*, 324-331.

Durand, A. (2007). Aqueous solutions of amphiphilic polysaccharides: concentration and temperature effect on viscosity. *European Polymer Journal*, *43*, 1744-1753.

Duxenneuner, M. R., Fischer, P., Windhab, E. J., & Cooper-White, J. J. (2008). Extensional properties of hydroxypropyl ether guar gum solutions. *Biomacromolecules*, *9*, 2989-2996.

Eggers, J. (1997). Nonlinear dynamics and breakup of free-surface flows. *Reviews of Modern Physics*, 69(3), 865-926.

Entov, V. M., & Hinch, E. J. (1997). Effect of a spectrum of relaxation times on the capillary thinning of a filament of elastic liquid. *Journal of Non-Newtonian Fluid Mechanics*, *72*, 31–54.

Gaume L. & Forterre Y. (2007). A Viscoelastic Deadly Fluid in Carnivorous Pitcher Plants. *PLoS ONE*, 2(11), e1185.
journal.pone.0001185

Gupta, R. K., Nguyen, D. A., & Sridhar, T. (2000). Extensional viscosity of dilute polystyrene solutions: Effect of concentration and molecular weight. *Physics of Fluids*, *12*, 1296-1318.

Haward, J. S., Sharma, V., Butts, C. P., Mckinley, G. H., & Rahatekar, S. S. (2012). Shear and extensional rheology of cellulose/ionic liquid solutions. *Biomacromolecules, 13*, 1688-1699.

Imeson, A. (2010). *Food stabilisers, thickeners and gelling agents*. Oxford, UK: Wiley-Blackwell.

Kulicke, W. M., Kiss, G., & Porter, R. S. (1977). Inertial normal-force corrections in rotational geometry. *Rheologica Acta*, *16*, 568-572.

Larson, G. (1988). *Constitutive Equations for Polymer Melts and Solutions.* Boston: Butterworths.

Launay, B., Cuvelier, G., & Salomon, M. R. (1997). Viscosity of locust bean, guar and xanthan gum solutions in the Newtonian domain: a critical examination of $\log(\eta_{sp})_o = \log C[\eta]_o$ master curves. *Carbohydrate Polymers*, *34*, 385-395.

Liang, R. F., & Mackley, M. R. (1994). Rheological characterization of the time and strain dependence for polyisobutylene solutions. *Journal of Non-Newtonian Fluid Mechanical*, *52*, 387-405.

Macosko, C. W. (1994). *Rheology: Principles, measurements, and applications*. New York: Wiley.

Marangoni, A. G., & Narine, S. S. (2002). *Physical properties of lipids*. Florida: CRC Press.

McKinley, G. H. (2005). Visco-elastic-capillary thinning and break-up of complex fluid. *Rheology Reviews (The British Society of Rheology)*, 1-49.

McKinley, G. H., & Tripathi, A. (2000). How to extract the Newtonian viscosity from capillary breakup measurements in a filament rheometer. *Journal of Rheology*, *44*, 653-670.

Meza, B. E., Chesterton, A. K. S., Verdini, R. A., Rubiolo, A. C., Sadd, P. A., Moggridge, G. D., & Wilson, D. I. (2011). Rheological characterisation of cake batters generated by planetary mixing: Comparison between untreated and heat-treated wheat flours. Journal of Food Engineering, *104*, 592-602.

Miquelim, J. N., & Lannes, S. C. D. S. (2009). Egg albumin and guar gum influence on foam thixotropy. *Journal of Texture Studies*, *40*, 623-636.

Moreira, R., Chenlo, F., & Torres, M. D. (2011). Rheological properties of commercial chestnut flour doughs with different gums. *International Journal of Food Science and Technology*, *46*, 2085 - 2095.

606 Moreira, R., Chenlo, F., Silva, C., Torres, M. D., Díaz-Varela, D., Hilliou, L., & Argence, H. (2012).
607 Surface tension and refractive index of guar and tragacanth gums aqueous dispersions at
608 different polymer concentrations, polymer ratios and temperatures. *Food Hydrocolloids*, *28*,
609 284-290.
610 Oblonsek, M., Sostar-Turk, S., & Lapasin, R. (2003). Rheological studies of concentrated guar gum.
611 *Rheologica Acta*, *42*, 491-499.
612 Odell, J. A., & Carrington, S. P. (2006). Extensional flow oscillatory rheometry. *Journal of Non-*
613 *Newtonian Fluid Mechanics*, *137*, 110-112.
614 Padmanabhan, M. (1995). Measurement of extensional viscosity of viscoelastic liquid foods. *Journal*
615 *of Food Engineering*, *25*, 311-327.
616 Renardy, M. (1994). Some comments on the surface-tension driven breakup or the lack of it of
617 viscoelastic jets. *Journal of Non-Newtonian Fluid Mechanical*, *51*, 97-107.
618 Renardy, M. (1995). A numerical study of the asymptotic evolution and breakup of Newtonian and
619 viscoelastic jets. *Journal of Non-Newtonian Fluid Mechanical*, *59*, 267–282.
620 Rosell, C. M., Collar, C., & Haros, M. (2007). Assessment of hydrocolloid effects on the thermo-
621 mechanical properties of wheat using the Mixolab. *Food Hydrocolloids, 21*, 454-462.
622 Steffe, J. F. (1996). *Rheological Methods in Food Process Engineering*, Michigan: Freeman Press.
623 Szyszkowski, B. (1908). Experimentelle Studien über kapillare Eigenschaften der wässrigen
624 Lösungen von Fettsäuren. *Zeitschrift für Physikalische Chemie*, *64*, 385-414.
625 Sittikijyothin, W., Torres, D., & Gonçalves, M. P. (2005). Modelling the rheological behaviour of
626 galactomannan aqueous solutions. *Carbohydrate Polymers*, *59*, 339-350.
627 Tembely M., Vadillo, D. C., Mackley, M. R., & Soucemarianadin, A. (2012). The matching of a
628 "one-dimensional" numerical simulation and experiment results for low viscosity Newtonian
629 and non-Newtonian fluids during fast filament stretching and subsequent break-up. *Journal of*
630 *Rheology*, *56*, 159-184.
631 Tatham, J. P., Carrington, S., Odell, J. A., Gamboa, A. C., Muller, A. J., & Saez, A. E. (1995).
632 Extensional behavior of hydroxypropyl guar solutions: Optical rheometry in opposed jets and
633 flow through porous media. *Journal of Rheology*, *39*, 961-986.
634 Torres, M. D., Gadala-Maria, F., & Wilson, D. I. (2013). Comparison of the rheology of bubbly
635 liquids prepared by whisking air into a viscous liquid (honey) and a shear-thinning liquid
636 (guar gum solutions). *Journal of Food Engineering*, *118*, 213-228.
637 Tuladhar, T. R., Mackley, M. R. (2008). Filament stretching rheometry and break-up behaviour of
638 low viscosity polymer solutions and ink jets fluids. *Journal of Non-Newtonain Fluid*
639 *Mechanics*, *148*, 97-108.
640 Vadillo, D. C., Mathues, W., & Clasen, C. (2012a). Microsecond relaxation processes in shear and
641 extensional flows of weakly elastic polymer solutions. *Rheologica Acta*, *51*, 755-769.

642 Vadillo, D. C., Tembely, M., Mackely, M. R., & Soucemarianadin, A. (2012b). The matching of
643 polymer solution fast filament stretching, relaxation, and break up experimental results with
644 1D and 2D numerical viscoelastic simulation. *Journal of Rheology*, *56*, 1491-1516.
645 Vadillo, D. C., Tuladhar, T. R., Mulji, A. C., Jung, S., Hoath, S. D., & Mackley, M. R. (2010).
646 Evaluation of the inkjet fluid's performance using the ''Cambridge Trimaster'' filament
647 stretch and break-up device. *Journal of Rheology*, *54*, 261-282.
648 Yesilata, B., Clasen, C. & McKinley, G. (2006). Nonlinear shear and extensional flow dynamics of
649 wormlike surfactant solutions. Journal of Non-Newtonain Fluid Mechanics, 133, 73-90.

Figure Captions

Figure 1 Effect of guar gum concentration on surface tension relative to water. Solid trend line shows Equation [12] fitted to the guar gum data with parameters a = 0.0123 and b = 0.0045 g/L. Experimental data showed high reproducibility and estimated uncertainty is smaller than symbol size.

Figure 2 Flow curves of aqueous guar gum solutions prepared at several concentrations. Symbols: circles – 1 g/L, triangles - 2 g/L, squares – 5 g/L, diamonds - 10 g/L, dashes – 15 g/L, crosses - 20 g/L. The solid line shows the best fit to the guar gum solutions obtained with the Cross model (Equation [2]), with parameters given in Table 1. In this and subsequent plots, error bars are not plotted if the uncertainty in data values is smaller than the symbol size.

Figure 3 Stress parameters measured for aqueous guar gum solutions prepared at different polymer concentration: (a) normal stress differences (N_1-N_2) and (b) estimated Weissenberg number (=(N1–N2)/τ). Symbols: circles – 1 g/L, triangles - 2 g/L, squares – 5 g/L, diamonds - 10 g/L, dashes – 15 g/L, crosses - 20 g/L.

Figure 4 Mechanical spectra of representative aqueous guar gum solutions prepared at concentrations of (a) 1, 5, (b) 10 and 20 g/L. Symbols: closed – G', open – G", circles – 1 g/L, squares – 5 g/L, diamonds - 10 g/L, triangles - 20 g/L. Solid and dashed lines in (b) shows G' and G" values for aqueous guar gum solution at 5g/L, respectively.

Figure 5 Comparison between the apparent viscosity (symbols) and the complex viscosity (dashed lines) for aqueous guar gum solutions prepared at several concentrations, Cox-Merz rule (Cox & Merz, 1958). Symbols: circles – 1 g/L, triangles - 2 g/L, squares – 5 g/L, diamonds - 10 g/L, dashes – 15 g/L, crosses - 20 g/L.

Figure 6 Dimensionless filament diameter profiles for aqueous guar gum solutions prepared at several concentrations. Symbols: circles – 1 g/L, triangles - 2 g/L, squares – 5 g/L, diamonds - 10 g/L, dashes – 15 g/L, crosses - 20 g/L. The non-linear profiles indicate non-Newtonian behaviour.

Figure 7 Correlation between time break-up (t_F) and polymer concentration (C) or initial filament diameter (D_1) for aqueous guar gum solutions prepared at several concentrations. Dashed lines show exponential trends: $t_F - t_{F0} = (1-e^{C/20})$ and $t_F = 15.2e^{0.0042D_i}$ (R^2 = 0.998).

Figure 8 Dimensionless filament diameter profiles with dimensionless time for aqueous guar gum solutions prepared at several concentrations. Symbols: circles – 1 g/L, triangles - 2 g/L, squares – 5 g/L, diamonds - 10 g/L, dashes – 15 g/L, crosses - 20 g/L.

Figure 9 Dimensionless filament diameter profiles with time for representative aqueous guar gum solutions prepared at 10 g/L. Dashed lines shows the fitting achieved with Equation [9] and solid lines with Equation [16].

Figure 10 Effect of polymer concentration on initial relaxation time (λ_1) and parameter b' (Equation [16]) for aqueous guar gum solutions prepared at several concentrations. Open symbols, λ_1; and closed symbols, b'. Dashed line shows the power-law trend obtained for λ_1 by Duxenneuner *et al.* (2008).

Figure 11 Correlation between initial relaxation time (λ_1) and break-up time (t_F) for aqueous guar gum solutions prepared at labelled concentrations. Dashed line shows linear trend, with $t_F = 8.06\lambda_1 - 34.3$ ($R^2 = 0.987$).

Figure 12 Extensional viscosity versus (a) Hencky strain and (b) polymer concentration (C) for aqueous guar gum solutions. Symbols: circles – 1 g/L, triangles - 2 g/L, squares – 5 g/L, diamonds - 10 g/L, dashes – 15 g/L, crosses - 20 g/L. Dashed line (maximum extensional viscosities) shows exponential trend, with $\eta_e = 5.4\ e^{0.035C}$ ($R^2 = 0.990$). Solid line (steady extensional viscosities) shows linear trend, with $\eta_e = 0.14C + 5.6$ ($R^2 = 0.995$).

Figure 13 Correlation between Trouton ratio and (a) Hencky strain and (b) polymer concentration for guar gum solutions. Symbols: circles – 1 g/L, triangles - 2 g/L, squares – 5 g/L, diamonds - 10 g/L, dashes – 15 g/L, crosses - 20 g/L. Dashed line in (b) shows the trend obtained by Duxenneuner *et al*. (2008). N_{TR} in (b) evaluated at 0.1 s^{-1}.

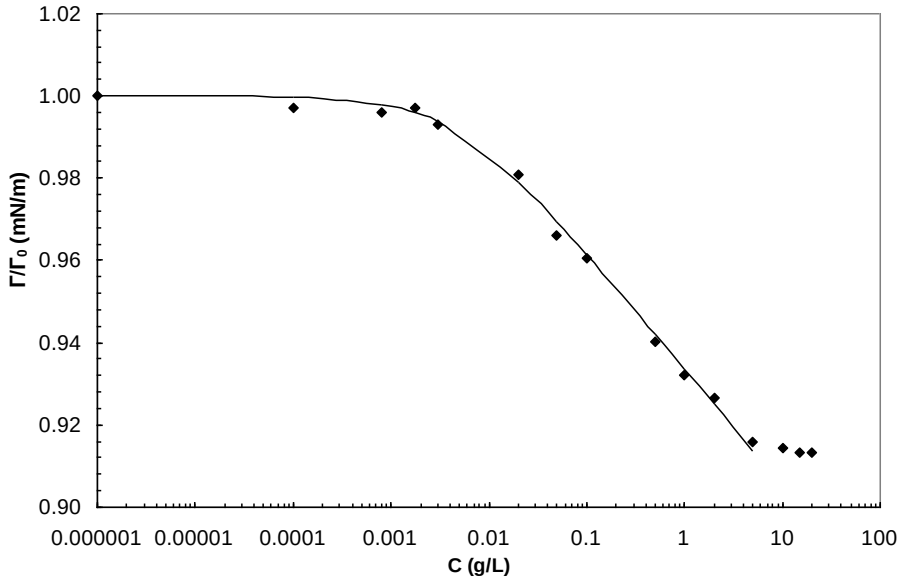

714
715

716 **Figure 1** Effect of guar gum concentration on surface tension relative to water. Solid trend line
717 shows Equation [12] fitted to the guar gum data with parameters a = 0.0123 and b = 0.0045
718 g/L. Experimental data showed high reproducibility and estimated uncertainty is smaller
719 than symbol size.

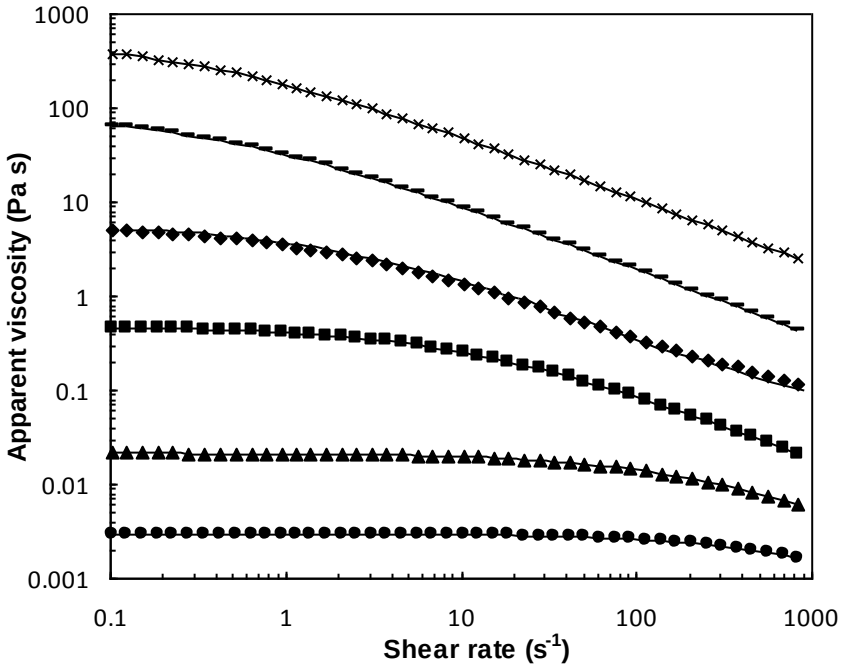

720

721

722 **Figure 2** Flow curves of aqueous guar gum solutions prepared at several concentrations. Symbols:
723 circles – 1 g/L, triangles - 2 g/L, squares – 5 g/L, diamonds - 10 g/L, dashes – 15 g/L,
724 crosses - 20 g/L. The solid line shows the best fit to the guar gum solutions obtained with
725 the Cross model (Equation [2]), with parameters given in Table 1. In this and subsequent
726 plots, error bars are not plotted if the uncertainty in data values is smaller than the symbol
727 size.

728

729 (a)

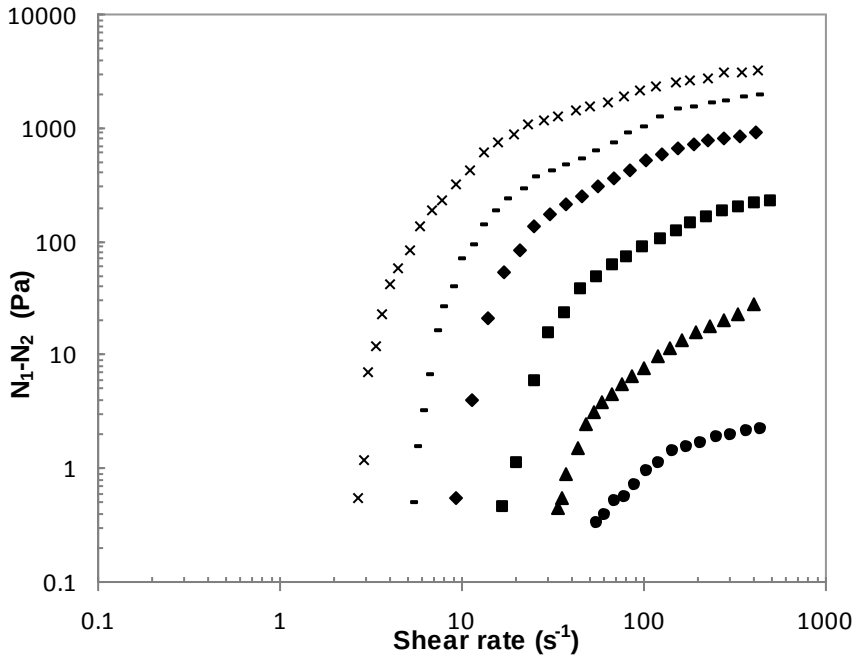

730

731 (b)

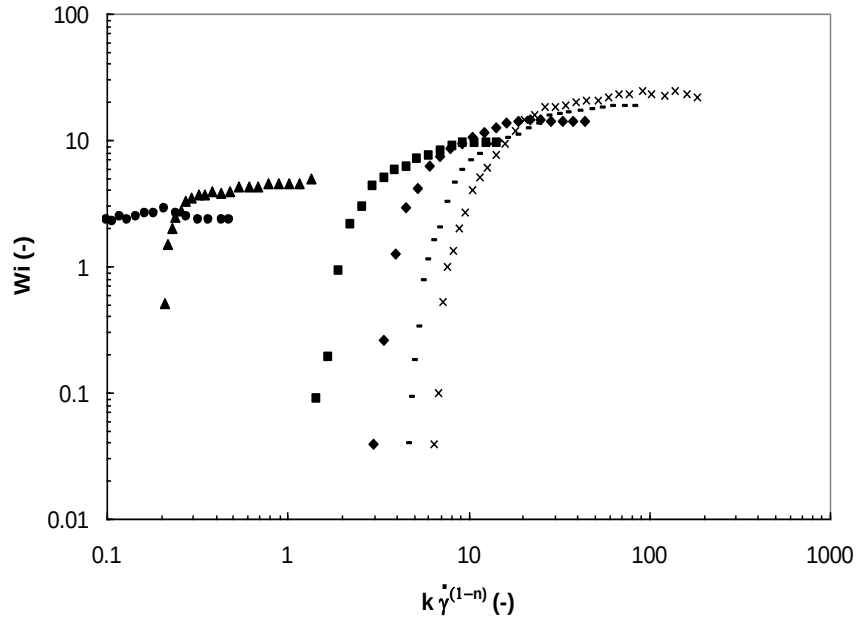

732

733 **Figure 3** Stress parameters measured for aqueous guar gum solutions prepared at different polymer
734 concentration: (a) normal stress differences (N_1-N_2) and (b) estimated Weissenberg number
735 (=(N1–N2)/τ). Symbols: circles – 1 g/L, triangles - 2 g/L, squares – 5 g/L, diamonds - 10
736 g/L, dashes – 15 g/L, crosses - 20 g/L.

(*a*)

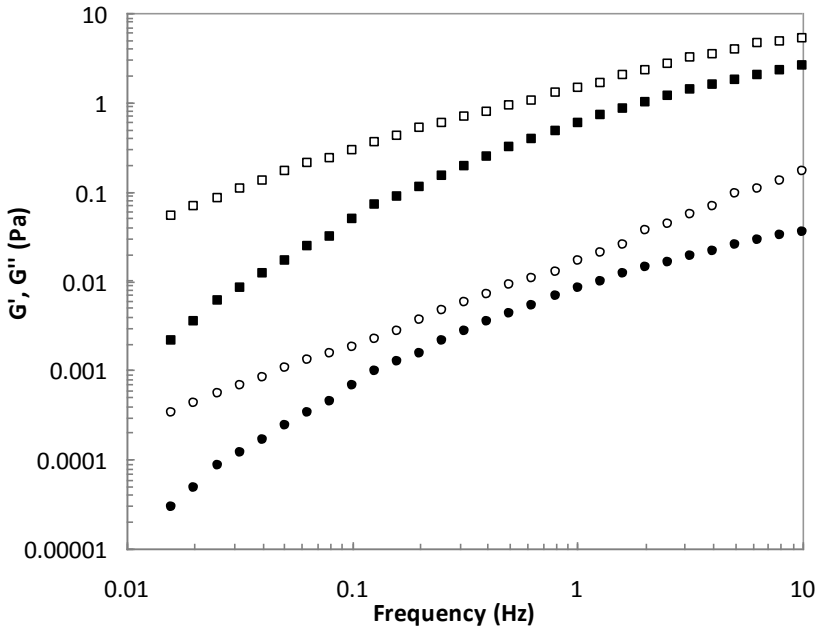

(*b*)

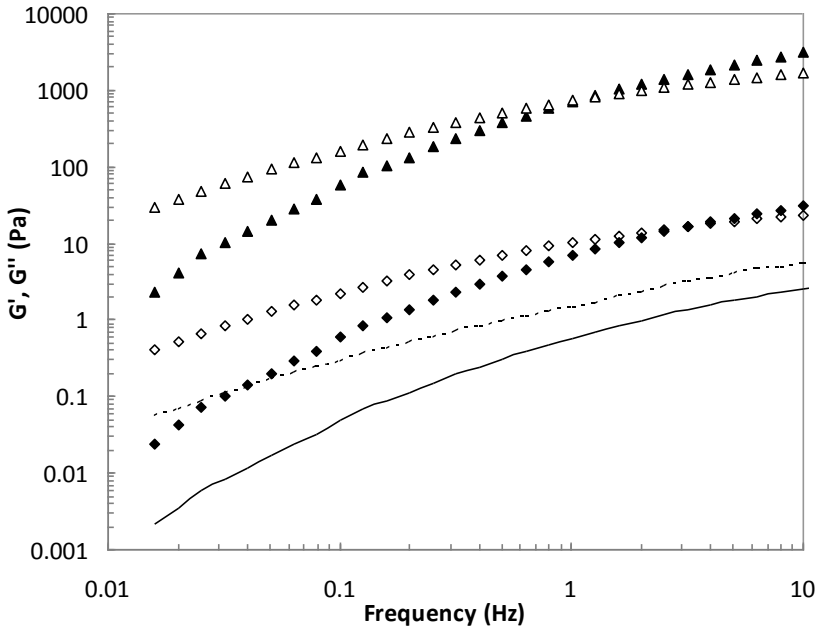

Figure 4 Mechanical spectra of representative aqueous guar gum solutions prepared at concentrations of (a) 1, 5, (b) 10 and 20 g/L. Symbols: closed – G', open – G", circles – 1 g/L, squares – 5 g/L, diamonds - 10 g/L, triangles - 20 g/L. Solid and dashed lines in (b) shows G' and G" values for aqueous guar gum solution at 5g/L, respectively.

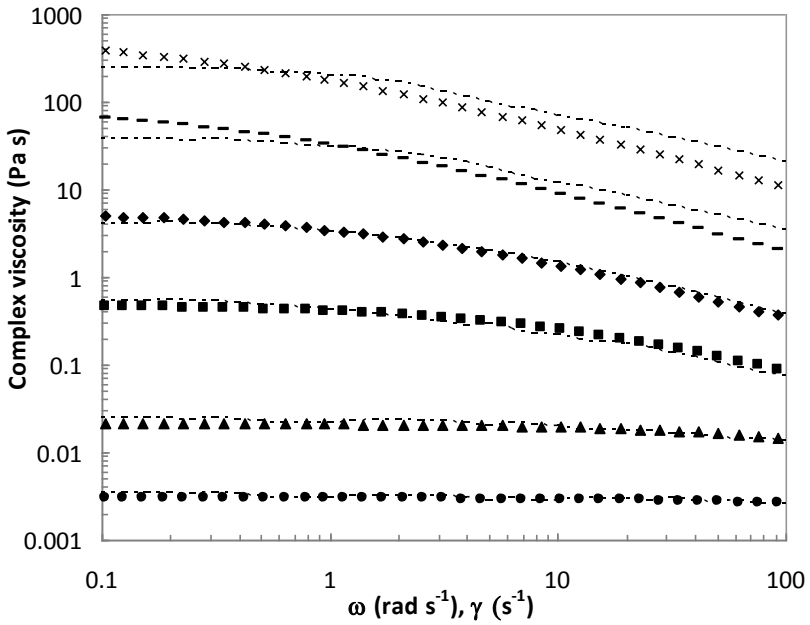

746

747

748 **Figure 5** Comparison between the apparent viscosity (symbols) and the complex viscosity (dashed
749 lines) for aqueous guar gum solutions prepared at several concentrations, Cox-Merz rule
750 (Cox & Merz, 1958). Symbols: circles – 1 g/L, triangles - 2 g/L, squares – 5 g/L, diamonds -
751 10 g/L, dashes – 15 g/L, crosses - 20 g/L.

752

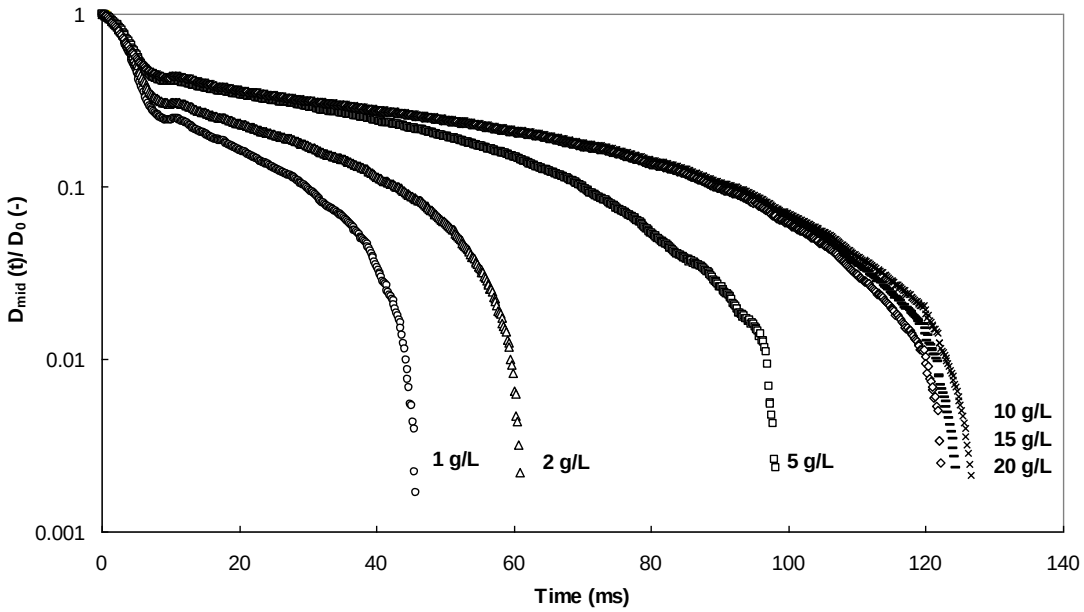

753

754

755 **Figure 6** Dimensionless filament diameter profiles for aqueous guar gum solutions prepared at
756 several concentrations. Symbols: circles – 1 g/L, triangles - 2 g/L, squares – 5 g/L,
757 diamonds - 10 g/L, dashes – 15 g/L, crosses - 20 g/L. The non-linear profiles indicate non-
758 Newtonian behaviour.

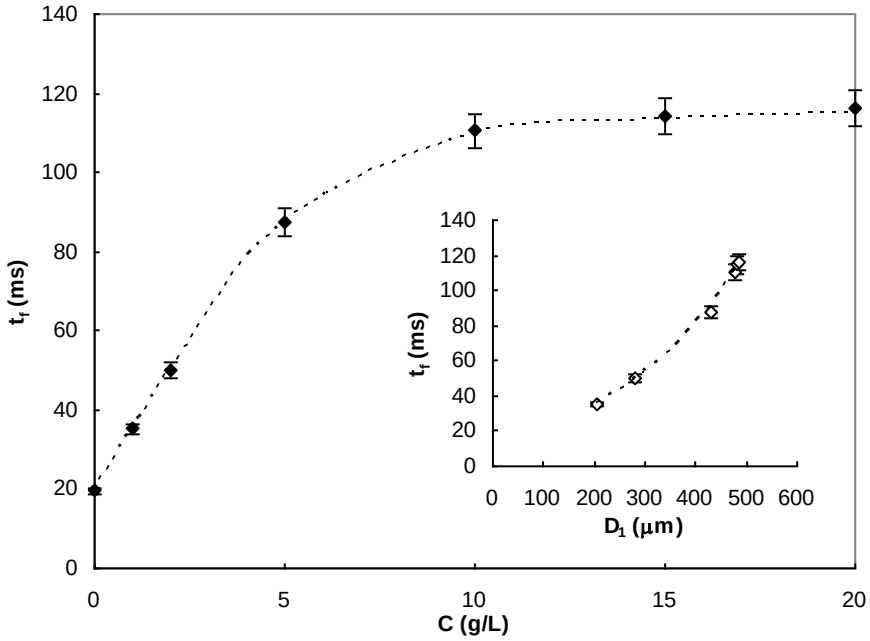

759
760

761 **Figure 7** Correlation between time break-up (t_F) and polymer concentration (C) or initial filament
762 diameter (D_1) for aqueous guar gum solutions prepared at several concentrations. Dashed
763 lines show exponential trends: $t_F - t_{F0} = (1-e^{C/20})$ and $t_F = 15.2e^{0.0042D_1}$ ($R^2 = 0.998$).

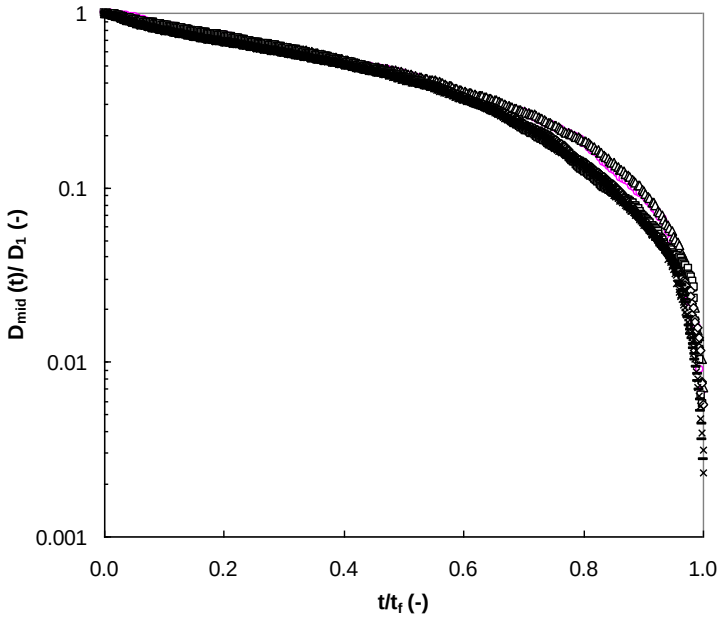

764
765

766 **Figure 8** Dimensionless filament diameter profiles with dimensionless time for aqueous guar gum
767 solutions prepared at several concentrations. Symbols: circles – 1 g/L, triangles - 2 g/L,
768 squares – 5 g/L, diamonds - 10 g/L, dashes – 15 g/L, crosses - 20 g/L.
769

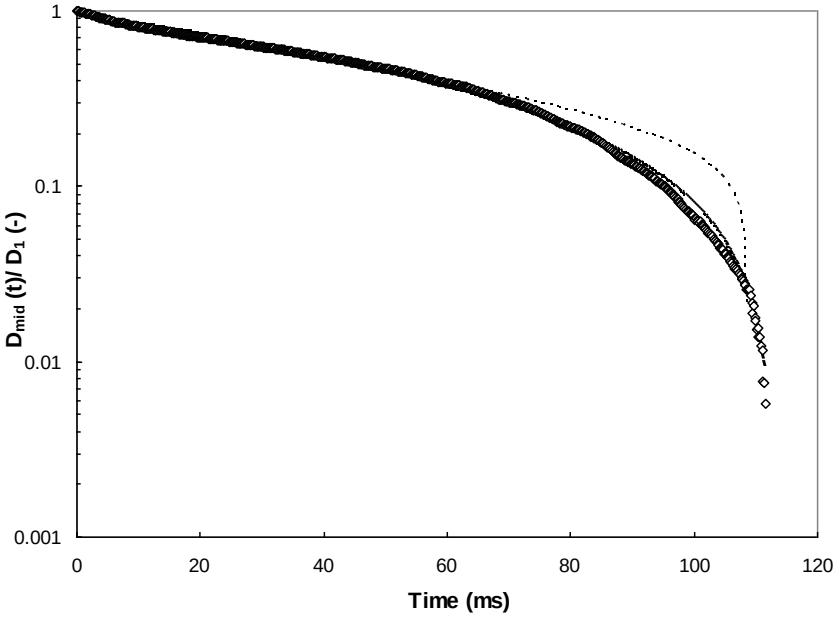

770
771
772 **Figure 9** Dimensionless filament diameter profiles with time for representative aqueous guar gum
773 solutions prepared at 10 g/L. Dashed lines shows the fitting achieved with Equation [9] and
774 solid lines with Equation [16].
775
776

(a)

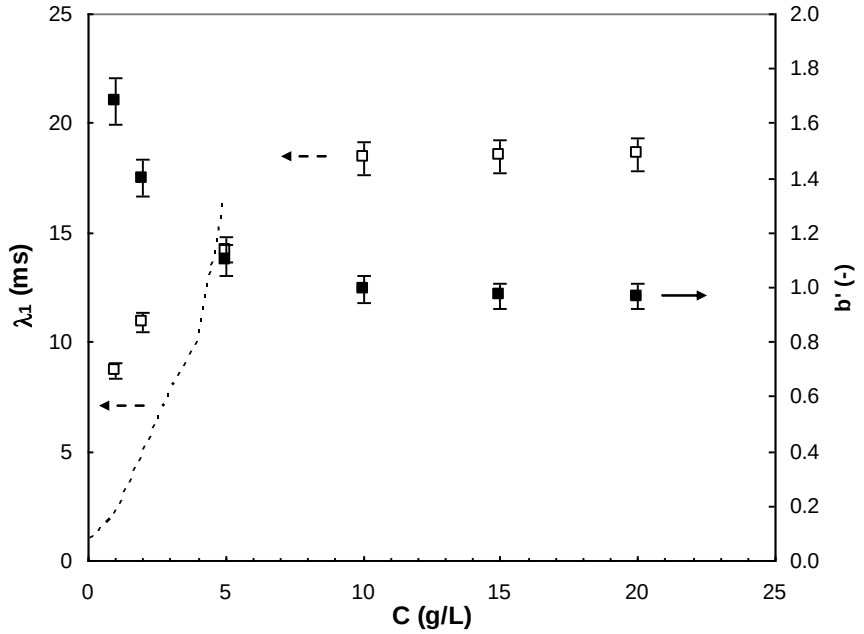

(b)

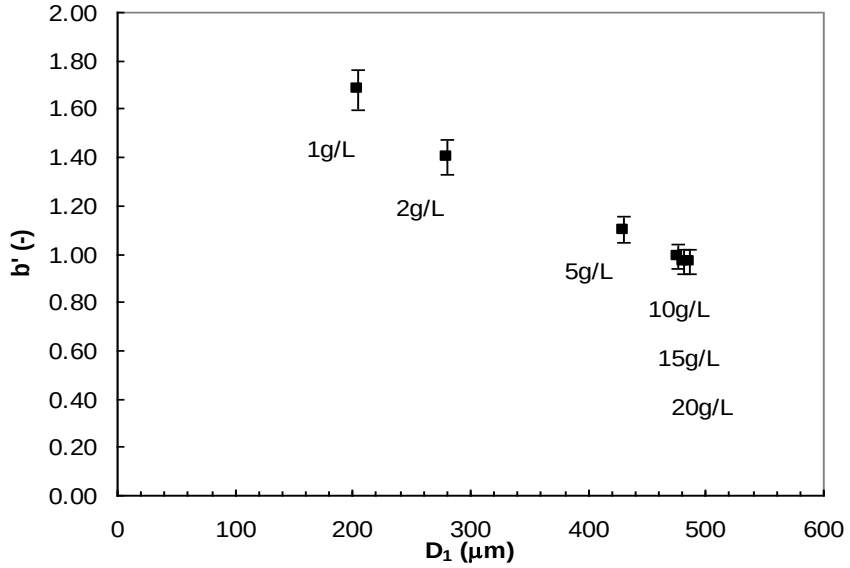

Figure 10 (a) Effect of polymer concentration on initial relaxation time (λ_1) and parameter *b*' (Equation [16]) for aqueous guar gum solutions prepared at several concentrations. Open symbols, λ_1; and closed symbols, *b*'. Dashed line shows the power-law trend obtained for λ_1 by Duxenneuner *et al.* (2008). (b) Relationship between parameter *b*' (Equation [16]) and filament formation diameter (D_1) for aqueous guar gum solutions prepared at several concentrations.

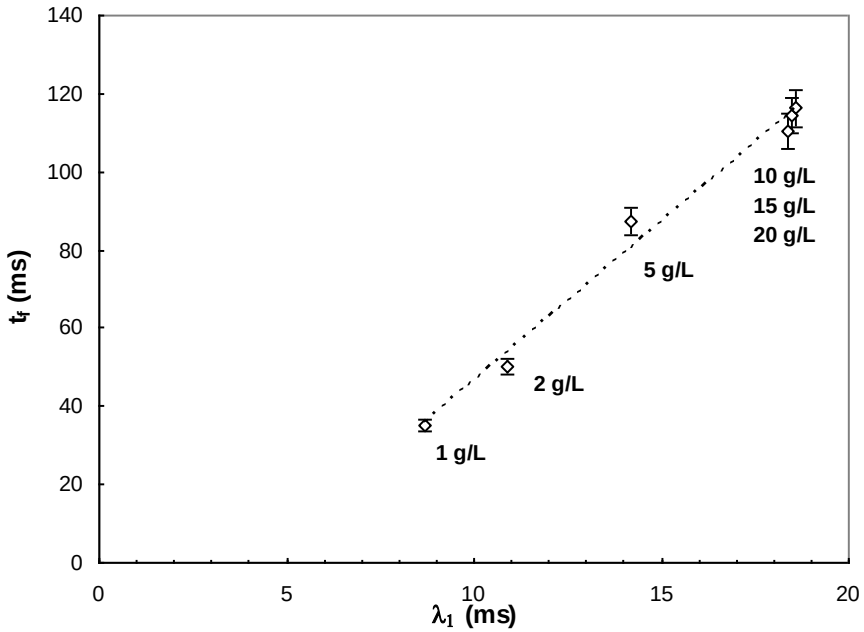

788
789
790 **Figure 11** Correlation between initial relaxation time (λ_1) and break-up time (t_F) for aqueous guar
791 gum solutions prepared at labelled concentrations. Dashed line shows linear trend, with t_F=
792 $8.06\lambda_1$ -34.3 (R^2 = 0.987).

(a)

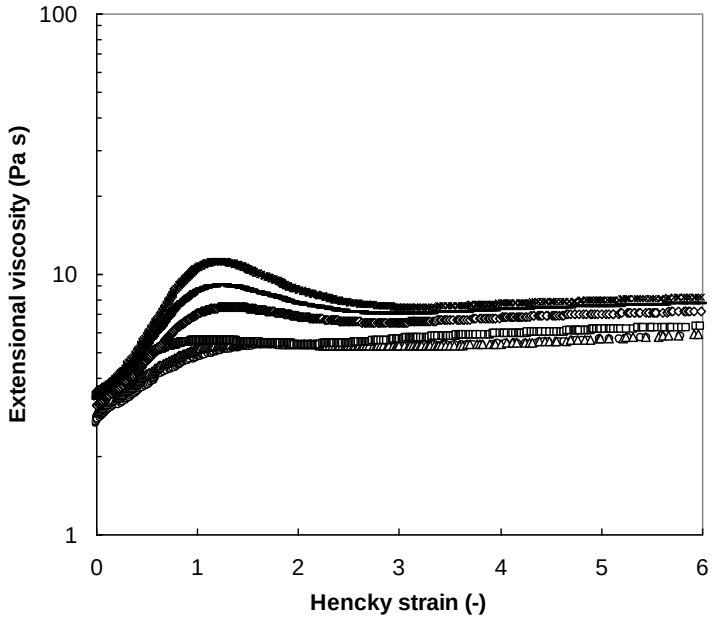

(b)

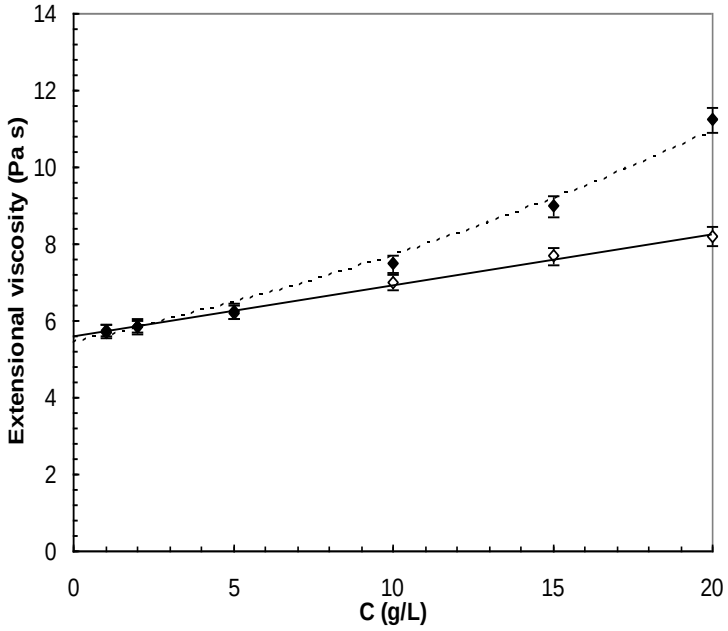

Figure 12 Extensional viscosity versus (a) Hencky strain and (b) polymer concentration (C) for aqueous guar gum solutions. Symbols: circles – 1 g/L, triangles - 2 g/L, squares – 5 g/L, diamonds - 10 g/L, dashes – 15 g/L, crosses - 20 g/L. Dashed line (maximum extensional viscosities) shows exponential trend, with $\eta_e = 5.4\ e^{0.035C}$ (R^2 = 0.990). Solid line (steady extensional viscosities) shows linear trend, with $\eta_e = 0.14C + 5.6$ (R^2=0.995).

802 (a)

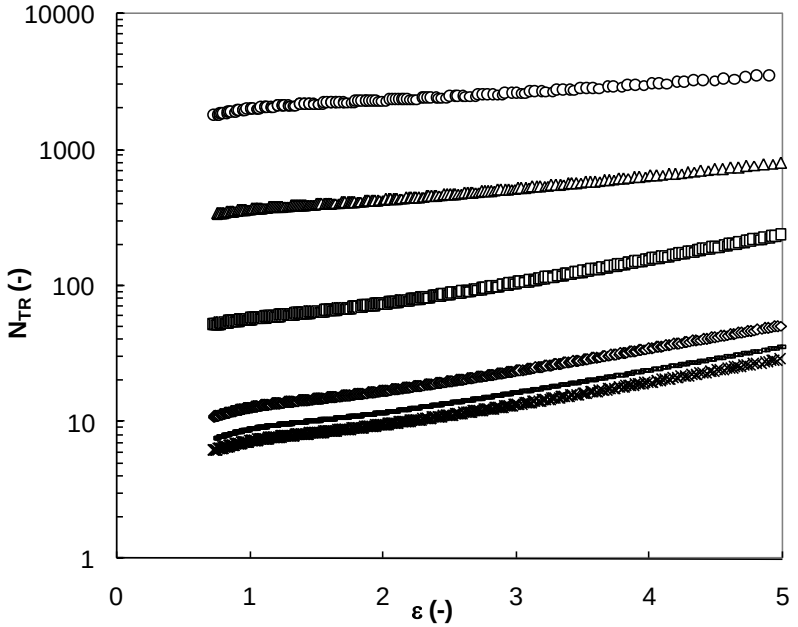

803

804 (b)

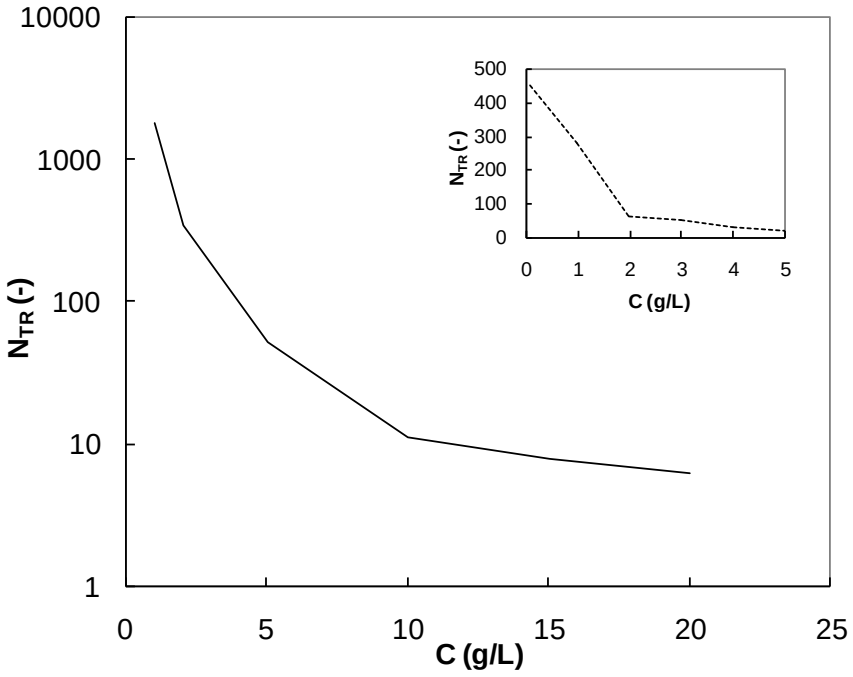

805

806 **Figure 13** Correlation between Trouton ratio and (a) Hencky strain and (b) polymer concentration
807 for guar gum solutions. Symbols: circles – 1 g/L, triangles - 2 g/L, squares – 5 g/L,
808 diamonds - 10 g/L, dashes – 15 g/L, crosses - 20 g/L. Dashed line in (b) shows the trend
809 obtained by Duxenneuner *et al*. (2008). N_{TR} in (b) evaluated at 0.1 s^{-1}.

Table Captions

Table 1 Parameter values obtained for Cross-Williamson model, Equation [2], for aqueous guar gum solutions prepared at several concentrations.

Table 1 Parameter values obtained for Cross-Williamson model, Equation [2], for aqueous guar gum solutions prepared at several concentrations. †

Concentration (g/L)	η_0 (Pa s)	k (s^{1-n})	n (-)	R^2	Standard deviation (Pa s)
1	0.0031 ± 0.0002^{f}	0.0045 ± 0.0002^{f}	0.23 ± 0.01^{c}	0.999	0.025
2	0.0215 ± 0.0001^{e}	0.015 ± 0.011^{e}	0.25 ± 0.01^{b}	0.998	0.027
5	0.48 ± 0.02^{d}	0.19 ± 0.01^{d}	$0.28 \pm 0.01^{a,b}$	0.999	0.026
10	5.87 ± 0.01^{c}	0.61 ± 0.01^{c}	0.29 ± 0.01^{a}	0.997	0.030
15	89.5 ± 2.3^{b}	1.81 ± 0.01^{b}	0.30 ± 0.01^{a}	0.996	0.032
20	550 ± 10.4^{a}	2.20 ± 0.01^{a}	0.31 ± 0.01^{a}	0.997	0.029

†Data are presented as mean ± standard deviation. Data values in a column with different superscript letters are significantly different at the $p \leq 0.05$ level.